Oscillating Relationship between the East Asian Winter Monsoon and ENSO

SHENGPING HE

Nansen-Zhu International Research Centre, Institute of Atmospheric Physics, and Climate Change Research Center, Chinese Academy of Sciences, and University of Chinese Academy of Sciences, Beijing, China

HUIJUN WANG

Nansen-Zhu International Research Centre, Institute of Atmospheric Physics, Chinese Academy of Sciences, Beijing, China

(Manuscript received 26 March 2013, in final form 19 July 2013)

ABSTRACT

This work investigates the interdecadal variations of the relationship between the El Niño–Southern Oscillation (ENSO) and the East Asian winter monsoon (EAWM), further explores possible mechanisms, and finally considers a recent switch in the ENSO–EAWM relationship. The 23-yr sliding correlation between the Niño-3.4 index and the EAWM index reveals an obvious low-frequency oscillation with a period of about 50 yr in the ENSO–EAWM relationship. Warm ENSO events during high-correlation periods are associated with an unusually weak East Asian trough, a positive phase of the North Pacific Oscillation (NPO), significant southerly wind anomalies along coastal East Asia, and warmer East Asian continent and adjacent oceans. However, there are no robust and significant anomalies in the EAWM-related circulation during low-correlation periods. Because of the southeastward shift of the Walker circulation, the area of anomalously high pressure in the western Pacific retreats south of 25°N, confining it to the region of the Philippine Sea. In this sense, the Pacific–East Asian teleconnection is not well established. Consequently, ENSO's impact on the EAWM is suppressed. Additionally, the low-frequency oscillation of the ENSO–EAWM relationship might be attributable to the combined effect of the Pacific decadal oscillation (PDO) and the Atlantic multidecadal oscillation owing to their modulation on the establishment of the NPO teleconnection. The observation of two full cycles of the ENSO–EAWM relationship, a transition to negative PDO in the early 2000s and an enhancement of the Walker circulation in the late 1990s, suggests a recovery of the ENSO–EAWM relationship.

1. Introduction

The East Asian winter monsoon (EAWM) is one of the most conspicuous climate systems found in the Northern Hemisphere during the boreal winter. It comprises the Siberian high, the East Asian trough, and the East Asian jet stream, which are located in the lower-, mid-, and upper troposphere, respectively. Among those factors influencing the EAWM, the Siberian high plays an important role in largely determining the strength of the EAWM. Owing to the strong radiative cooling induced by Eurasian continental snow cover during winter, a huge cold high pressure system, which is the Siberian high, forms over northern Mongolia (Watanabe and Nitta 1999; Jeong et al. 2011). Along the eastern flank of the Siberian high, a strong northwesterly bifurcates to the south of Japan; one stream flows directly eastward toward the subtropical North Pacific, and the other flows along the east coast of East Asia (Lau and Li 1984; Wang and Chen 2010). This dry cold northwesterly wind often brings a severe cold surge and heavy snowfall events to East Asia (Boyle and Chen 1987; Chang et al. 2006; Wei et al. 2011; Li and Wang 2012a,b, 2013). In tandem with the development of the Siberian high, the East Asian jet stream in its core region becomes strong and the zonal wind speed in the south and north of the core region becomes weak, leading to the enhancement of anomalous cyclonic vorticity over East Asia. Thus, the East Asian trough develops and cold surges often occur (Holton 1992; Jhun and Lee 2004; Li and Yang 2010). In this way, the EAWM can exert strong influence on the winter climate in both Asia and other more remote

Corresponding author address: Shengping He, Nansen-Zhu International Research Centre, Institute of Atmospheric Physics, Chinese Academy of Sciences, Huayanli 40 Street, Chaoyang District, Beijing 100029, China.
E-mail: hshp@mail.iap.ac.cn

DOI: 10.1175/JCLI-D-13-00174.1

regions (Chang and Lau 1982; Ding and Krishnamurti 1987; Chang et al. 2006). In January 2008, severe cold waves and snowstorms affected southern China, causing profound social impact and huge economic losses (Wang et al. 2011).

Given its complexity and importance, great efforts have been made to study and explain the EAWM. In earlier studies, climatologists applied mainly statistical and diagnostic methods to reveal the relationship between the Siberian high and cold waves over East Asia (Ding and Krishnamurti 1987; Guo 1994). As knowledge about the EAWM has become more developed, researchers have realized that many other factors could influence the variability of the EAWM. For example, the impact on the EAWM of the Northern Hemisphere annular mode (NAM; also known as the Arctic Oscillation/North Atlantic Oscillation), proposed by Thompson and Wallace (1998), has been extensively studied. Wu and Huang (1999) noted that the Siberian high and the EAWM are weakened when the NAM is in its positive phase. Gong et al. (2001) revealed a significant out-of-phase relationship between the NAM and the EAWM and highlighted further that the impact of the NAM on the EAWM could be transmitted by the Siberian high. However, a significant negative NAM–EAWM relationship has also been documented by B. Wu and Wang (2002), who argued that the winter NAM and the Siberian high are relatively independent of each other in their influence on the EAWM. The Aleutian low, which can contribute to the west–east sea level pressure gradient for the EAWM, also shows an apparent relation to the NAM (Overland et al. 1999; Sun and Wang 2006). Thompson and Wallace (2000) indicated that the zonal component of anomalous flow associated with the NAM could induce temperature advection, which plays a key role in establishing and maintaining the stationary wave pattern. Chen and Huang (2002) found that the quasi-stationary planetary waves between the troposphere and the stratosphere could be modulated significantly by the NAM, and thus the NAM–EAWM relationship could be interpreted from the perspective of quasi-stationary planetary waves (Chen et al. 2005). According to their study, when the NAM is in its positive phase, there are more quasi-stationary planetary waves propagating from high latitudes to lower latitudes, and there exists a smaller perturbation in the polar vortex. At the same time, the Siberian high, the Aleutian low, the East Asian jet stream, and the East Asian trough all weaken, which leads to a weak EAWM.

The El Niño–Southern Oscillation (ENSO) phenomenon is thought to be an important forcing for the EAWM (Wang 2006). Li (1990) found that the anomalous atmospheric circulation in winter, induced by El Niño events, could lead to a weaker winter monsoon and that the anomalously stronger EAWM would in turn result in an El Niño event. Zhang et al. (1996) suggested that El Niño events could suppress convective activities over the western equatorial Pacific, which exerts significant impact on the monsoon-related circulation in this region. As a result, a southerly wind anomaly appears in the lower troposphere along the coast of East Asia, and a weak EAWM is favored. In addition, the interannual variation of winter northerlies near the South China Sea is well correlated with ENSO; strong (weak) northerly winds are generally associated with La Niña (El Niño) and years of high (low) Southern Oscillation (Zhang et al. 1997). A study by Wang et al. (2000) indicated that ENSO exerts an influence on the EAWM through a Pacific–East Asian teleconnection. During an El Niño winter, cyclonic vorticity emerges over the central tropical Pacific, emanating northwestward toward East Asia. Subsequently, an anticyclone and cyclonic vorticity form over the western North Pacific and northeast Asia, respectively. Thus, the anomalous southwesterlies prevailing to the northwest of the western North Pacific anticyclone are favorable for a weaker EAWM. Using the most recent version of the European Centre for Medium-Range Weather Forecasts (ECMWF) atmospheric general circulation model, Gollan et al. (2012) examined the tropical impact on the EAWM, and their experiments suggest a strong influence of the tropical circulation on the interannual variability of the EAWM.

However, an interdecadal climate shift has occurred since 1976, characterized by cooling sea surface temperature (SST) anomalies (SSTAs) in the central and western North Pacific and warming SST anomalies in the eastern tropical Pacific (Trenberth 1990; Deser et al. 1996) and intensification and eastward shift of the Aleutian low (Graham 1994; Trenberth and Hurrell 1994) in the North Pacific in the mid-1970s. A significant southeastward shift in the centers of anomalous subsidence and rising motion is also observed in the Walker circulation in the late 1970s (Kumar et al. 1999). Meanwhile, the relationships between ENSO and many other climate systems change a great deal. For example, the inverse relationship between ENSO and the Indian summer monsoon has broken down in recent decades (Kumar et al. 1999), and the East Asian summer monsoon circulation related to ENSO has also experienced a remarkable change (Wang 2001; Wang 2002; R. Wu and Wang 2002). Wang (2002) demonstrated the existence of instability in the relationship between the East Asian summer monsoon and ENSO. Similarly, the link between ENSO and the EAWM is also not static. As identified by Zhou et al. (2007b), the EAWM and ENSO are not consistently highly correlated and their relationship clearly undergoes low-frequency oscillation.

This nonrobust ENSO–EAWM relationship might be modulated by the phase of the Pacific decadal oscillation (PDO) (Wang et al. 2008, hereafter WCH08). Recently, He et al. (2013) revealed that since the 1970s the impact of ENSO on the East Asian–western North Pacific circulation has weakened, while its impact on the eastern North Pacific–North American circulation has strengthened. Meanwhile, the relationship between the EAWM and ENSO has also weakened since the mid-1970s (Wang and He 2012).

ENSO is still the most predictable climatic signal (Kirtman and Schopf 1998; Cheng et al. 2011; Sun and Wang 2012), and the weakening of the ENSO–EAWM relationship might present greater challenges for winter climate prediction. However, according to previous studies, it is still unclear whether the EAWM–ENSO relationship will remain tenuous or recover in the future. The reasons for this are 1) in the studies of He et al. (2013) and Wang and He (2012), the period of interest is too short to determine whether there exists a cycle in the ENSO–EAWM relationship; 2) even though Zhou et al. (2007b), who focused on the relationship on a decadal time scale, documented the low-frequency oscillation of the ENSO–EAWM relationship by analyzing datasets over longer periods, no regular periodic cycle was determined; and 3) WCH08 found that the ENSO–EAWM relationship might be modulated by the PDO, which shows two general periodicities: one from 15 to 25 yr and the other from 50 to 70 yr (Mantua et al. 1997). However, we are not convinced whether it is true for a longer period because their main results were derived from the 40-yr ECMWF Re-Analysis (ERA-40) dataset. Generally, there are two options available in projecting future climate. One is model simulations, which are widely used in phases 3 and 5 of the Coupled Model Intercomparison Project (please see http://cmip-pcmdi.llnl.gov/). The other is diagnostic analysis of historical climate, which is of great benefit in building a statistical model.

In this study, we use the diagnostic analysis method to investigate the long-term variability of the relationship between ENSO and the EAWM during the winters of 1871–2009. Consistent with the previous studies cited above, we found that the interannual ENSO–EAWM relationship, which weakened in the 1970s and might be modulated by the PDO, undergoes low-frequency oscillation. Of course, some new results have also been obtained. First, the ENSO–EAWM relationship shows a regular quasi-50-yr low-frequency oscillation. Second, some factors other than the PDO [e.g., the Atlantic multidecadal oscillation (AMO)] might also modulate the oscillation of the ENSO–EAWM relationship. Third, a recent recovery of the ENSO–EAWM relationship is proposed based on the present analysis. Additionally, we offer new interpretations on why the ENSO–EAWM relationship adopts a weak–strong cycle. These include the shift of the Walker circulation and its impact on the establishment of the Pacific–East Asia teleconnection (PEAT), as proposed by Wang et al. (2000), and the combined effect of PDO and AMO in reducing the meridional pressure gradient during El Niño years being conducive to a significantly weaker EAWM.

2. Data and methods

The datasets used in this study include 1) monthly-mean sea level pressure (SLP), winds at 850 hPa, and geopotential height at 500 hPa (H500) derived from the Twentieth Century Reanalysis, version 2, data (1871–2009) (Compo et al. 2011) provided by the National Oceanic and Atmospheric Administration (NOAA) website (at http://www.esrl.noaa.gov/psd/); and 2) monthly-mean SST obtained from the NOAA extended reconstructed SST, version 3, analysis (1854–2012) (Smith et al. 2008).

Besides, the monthly-mean surface air temperature (SAT), SLP, 850-hPa wind, and H500 of the National Centers for Environmental Prediction–U.S. Department of Energy (NCEP–DOE) Reanalysis 2 (1979–2012) (Kanamitsu et al. 2002), obtained from their website (at http://www.esrl.noaa.gov/psd/data/gridded/data.ncep.reanalysis2.html), is also used. To support the results derived from the reanalysis datasets, two observational datasets are introduced. One is the high-resolution gridded near-surface temperature from Climate Research Unit (CRU TS3.1), with a resolution of 0.5° by 0.5° (Mitchell and Jones 2005) (obtained from http://www.cru.uea.ac.uk/cru/data/hrg/). The other is the Hadley Centre sea level pressure dataset (HadSLP2r), with a resolution 5° by 5° (Allan and Ansell 2006) (obtained from http://www.esrl.noaa.gov/psd/gcos_wgsp/Gridded/data.hadslp2.html).

Several climatic indices are used to facilitate the analysis, including 1) the EAWM index, which is defined as the negative area-averaged winter 500-hPa geopotential height within the domain of 25°–45°N and 110°–145°E, where the East Asian trough is located and can reflect well the variations of the EAWM-related temperature and circulation (Sun and Li 1997; Wang et al. 2009; He and Wang 2012); 2) the Aleutian low index, which is defined as the winter SLP averaged within 30°–70°N and 155°E–130°W (He and Wang 2012); 3) the North Pacific Oscillation (NPO) index, which is defined as the principal component of the leading mode of the empirical orthogonal function (EOF) analysis for the standardized winter SLP over the North Pacific (20°–80°N, 120°E–120°W) (Overland et al. 1999); 4) the Niño-3.4 index, which is defined as the area-averaged

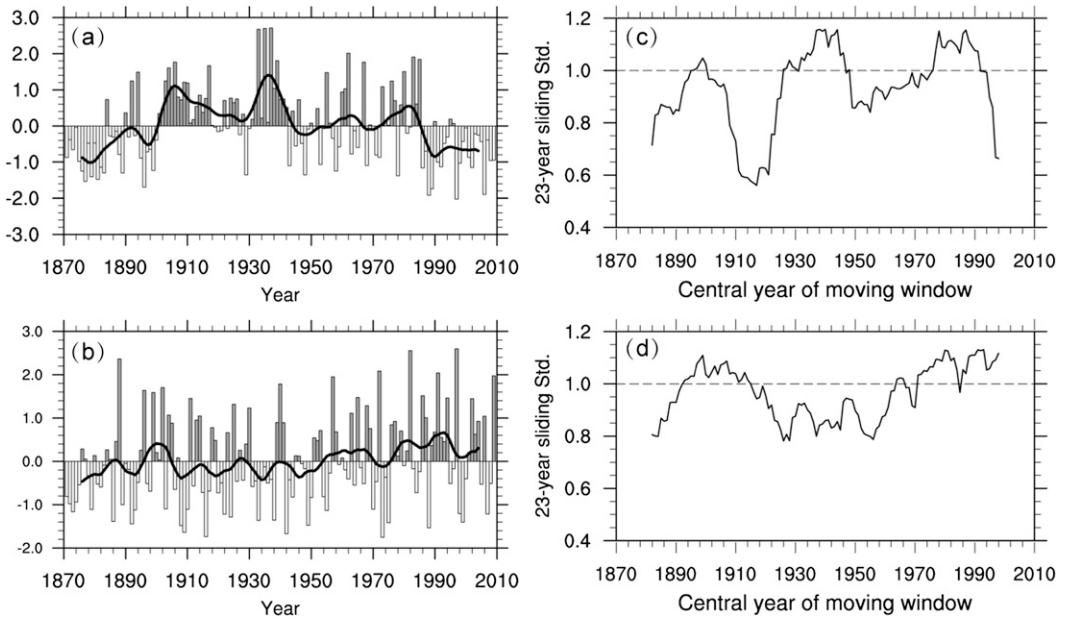

FIG. 1. The normalized (bars) and 11-yr running mean (line) of the (a) East Asian winter monsoon index (EAWMI) and (b) Niño-3.4 index for 1871–2009 winters together with 23-yr sliding standard deviation of (c) EAWMI and (d) Niño-3.4 index.

SSTAs in the Niño-3.4 region (5°S–5°N, 120°–170°W); and 5) the Pacific–North American (PNA) index, which is obtained from the NCEP Climate Prediction Center (http://www.cpc.ncep.noaa.gov/products/precip/CWlink/pna/pna.shtml). In this study, the winter [December–February (DJF)] of 1900 refers to December 1899, January 1900, and February 1900. To emphasize the interannual variability, an 11-yr high-pass filter is applied to obtain the interannual anomalies of the aforementioned data.

3. Oscillation of the ENSO–EAWM relationship

As shown in Fig. 1a, the EAWM is composed of both interannual and interdecadal variability. From the 11-yr running mean we observe four epochs (1871–1900, 1942–59, 1961–72, and 1986–2009) during which the EAWM is weaker than normal and two epochs (1901–41 and 1973–85) when the EAWM is stronger than normal. It should be noticed that the transition starting around the mid-1980s, after which the EAWM became weaker, is consistent with the previous studies of Chen et al. (2000) and Chang et al. (2006). Similarly, the ENSO index also has three below-normal epochs (1870–94, 1905–53, and 1970–75) and three above-normal epochs (1895–1904, 1954–69, and 1977–2009) (Fig. 1b). It appears that the interdecadal components of the EAWM and ENSO are not always concurrent. For example, they are almost in phase during 1870–1904, but mainly out of phase during 1905–40 and 1986–2009. Furthermore, their interannual components take on low-frequency oscillation, but with different periods (Figs. 1c,d). Figure 2 suggests that ENSO and the EAWM might covary in the time frequency of 2–7 and 16–32 yr. These facts raise a question about whether a low-frequency oscillation exists in the interannual relationship between the EAWM and ENSO. To address this, in Fig. 3 we present the 23-yr sliding correlation between the Niño-3.4 index and the EAWM-related indices.

As illustrated by Fig. 3a, the relationship between ENSO and the EAWM-related circulation is not stationary; high correlations alternate with low correlations throughout the entire period of 1871–2009. In addition to the weakening of the relationship that occurred in about 1976, which has been demonstrated by Wang and He (2012), another weakening occurred in about 1927, and two periods of strengthening appeared around 1900 and 1952. This means that the ENSO–EAWM relationship seems consistently highly correlated during 1900–26 and 1952–76 but is disrupted during 1927–51 and 1977–98. The Morlet wavelet indicates that the interannual relationship between ENSO and the EAWM has clearly undergone low-frequency oscillation in the past century with a period of about 50 yr (Figs. 3b,c).

Using the NCEP–DOE and ERA-40 reanalysis datasets, He et al. (2013) revealed that the evolution of the relationship between ENSO and the EAWM-related circulation is opposite to that of the relationship between

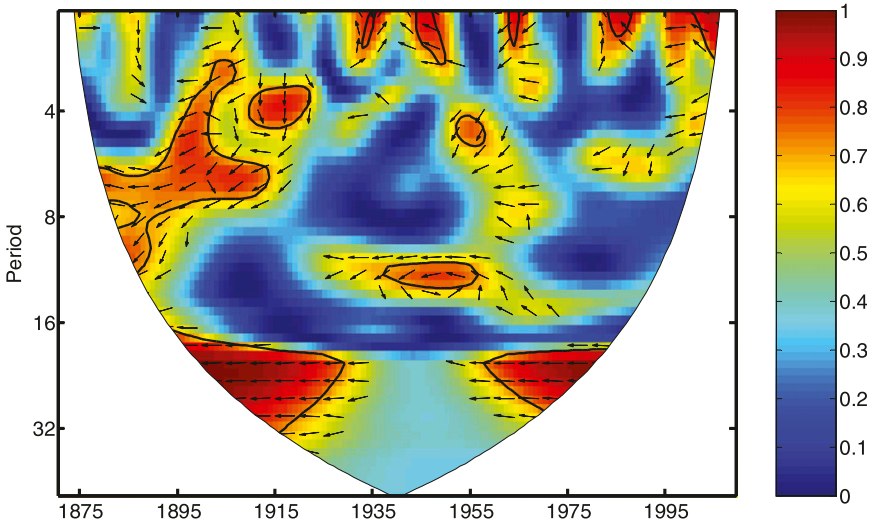

FIG. 2. Wavelet coherence between the standardized winter Niño-3.4 index and EAWMI for 1871–2009 winters. The values exceeding the 95% significant level are shown within the thick contour. The relative phase relationship is shown as arrows (with in-phase pointing right and antiphase pointing left). The software is provided by Aslak Grinsted (available online at http://noc.ac.uk/using-science/crosswavelet-wavelet-coherence).

ENSO and the eastern Pacific–North American circulation (i.e., the Aleutian low, PNA teleconnection) during 1958–2001. Based on their results, another issue we want to address is how the correlation between ENSO and the eastern Pacific–North American circulation changes over a longer period. Figure 4a shows the 23-yr sliding correlation of the Niño-3.4 index with the Aleutian low index (ALI; solid curve) and the PNA index (PNAI; dashed curve). Clearly, a significant in-phase relationship exists between ENSO and the Aleutian low during

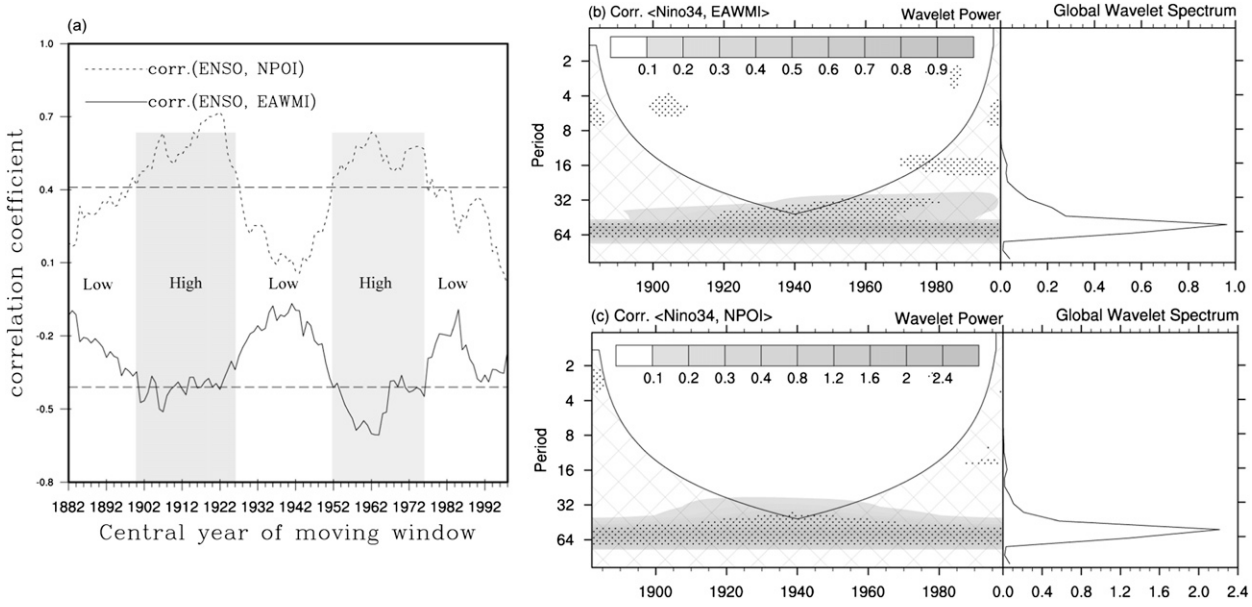

FIG. 3. (a) The 23-yr sliding correlation between the winter Niño-3.4 index and EAWMI (solid curve) and NPOI (dashed curve). The horizontal dashed lines indicates the 95% significant level. The Morlet wavelet of 23-yr sliding correlation of the Niño-3.4 index with (b) EAWMI and (c) NPOI. The left and right panels in (b) and (c) are local wavelet spectrum and global wavelet spectrum, respectively. The left axis is the Fourier period (yr) and the bottom axis is time (yr). The dotted regions are significant at the 95% level for a red noise process. Cross-hatched regions on either end indicate the ''cone of influence,'' where edge effects become important. Wavelet software was provided by C. Torrence and G. Compo (available online at http://paos.colorado.edu/research/wavelets/).

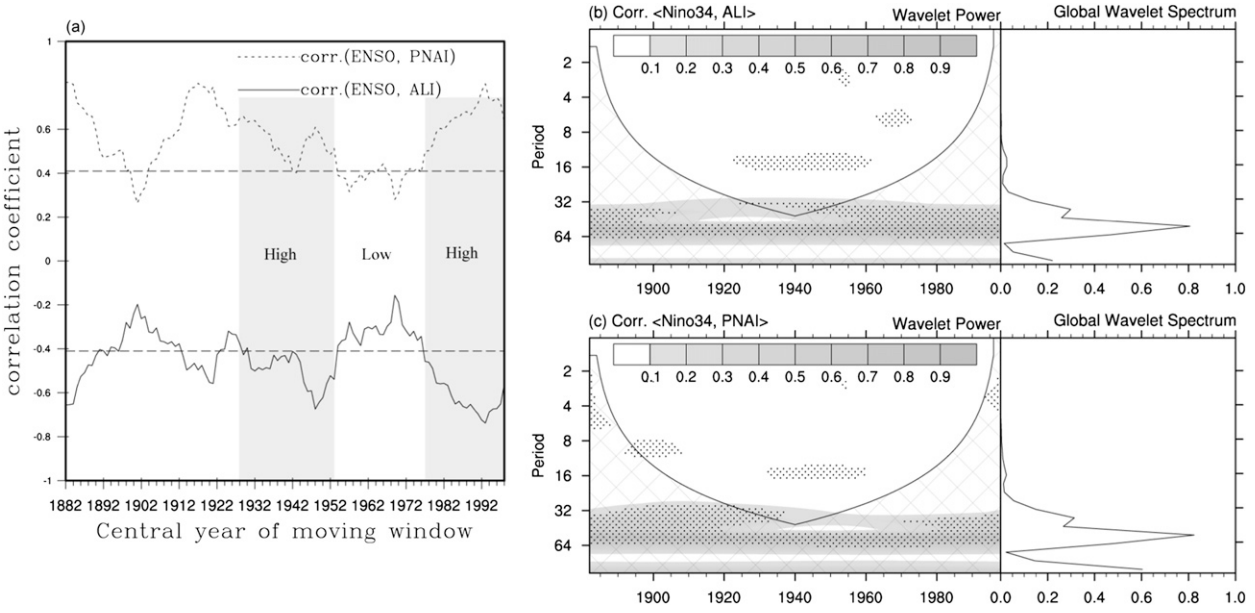

FIG. 4. (a) The 23-yr sliding correlation between the winter Niño-3.4 index and ALI (solid curve) and PNAI (dashed curve). The horizontal dashed lines indicates the 95% significant level. (b),(c) As in Figs. 3b,c, but for the Morlet wavelet of 23-yr sliding correlation of the Niño-3.4 index with the ALI and PNAI, respectively.

1882–96, 1902–53, and 1977–98, whereas an insignificant relationship appears during 1952–76. Meanwhile, ENSO and the PNA teleconnection are significantly negatively correlated during 1882–96, 1912–22, 1927–53, and 1977–98, but experience a weakening during the 1890s–1900s and 1954–76. The Morlet wavelet indicates that the interannual relationship between ENSO and the Aleutian low/PNA also takes on a low-frequency oscillation with a period of about 16 yr and a period of about 50 yr (Figs. 4b,c). It should be pointed out that the low-frequency oscillation is not sensitive to the sliding widow chosen. Given that the low-frequency oscillation of the ENSO–EAWN relationship, we take four sub periods, each comprising 25 yr (1902–26, 1927–51, 1952–76, and 1977–2001), to document the spatial differences of atmospheric circulation anomalies associated with the interdecadal change in the ENSO–EAWM relationship.

We compare the spatial distribution of the correlation between the Niño-3.4 index and the 500-hPa geopotential height anomalies among the four subperiods in Fig. 5.

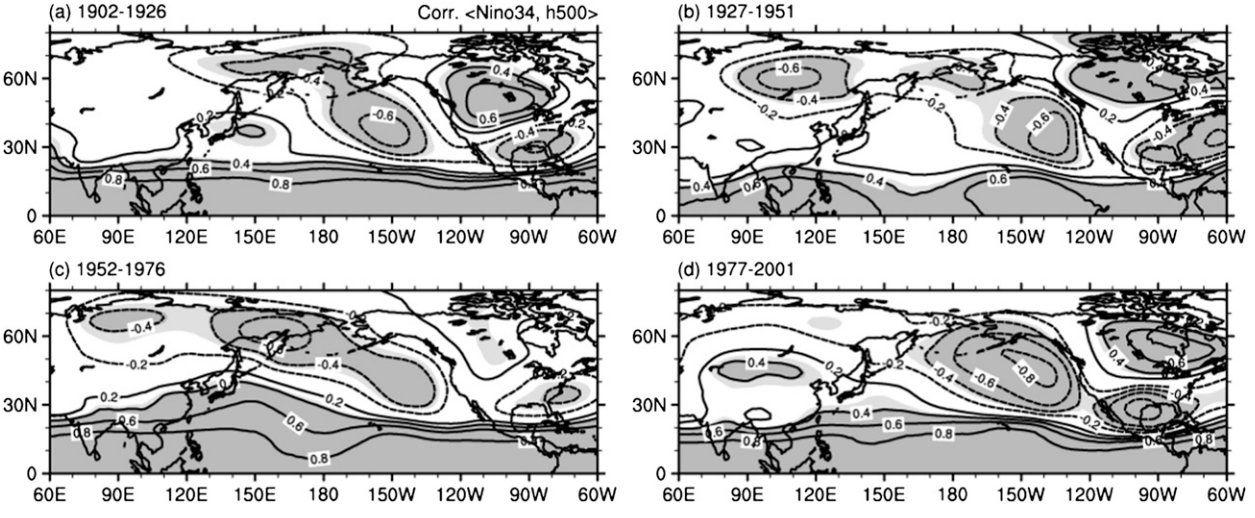

FIG. 5. Correlation coefficients between Niño-3.4 index and 500-hPa geopotential height anomaly for (a) 1902–26, (b) 1927–51, (c) 1952–1976, and (d) 1977–2001 winters, respectively. Light and dark shaded values are significant at the 90% and 95% level from a two-tailed Student's *t* test, respectively.

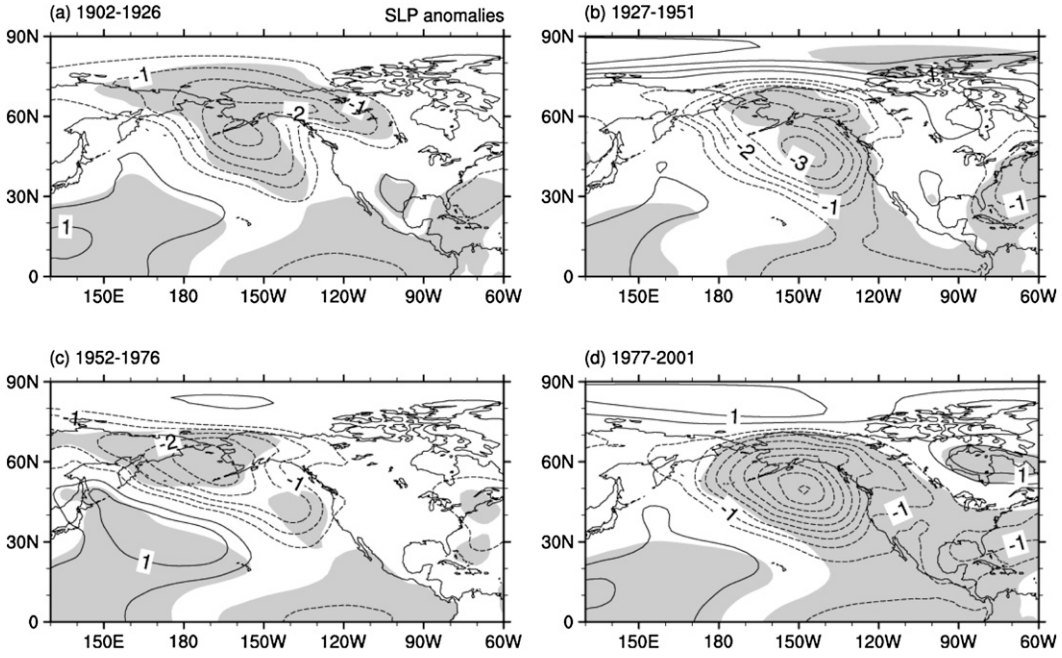

FIG. 6. Regression maps of winter sea level pressure anomalies with respect to the winter Niño-3.4 index for (a) 1902–26, (b) 1927–51, (c) 1952–76, and (d) 1977–2001 winters, respectively. The contour interval is 0.5 hPa and shaded values are significant at the 90% level from a two-tailed Student's *t* test.

Consistent with Figs. 3 and 4, the correlation pattern poleward of 20°N shows remarkable distinctions in different periods. During 1927–51, significant negative correlations are located in central Russia, the eastern North Pacific, and southeastern North America and its adjacent oceans, together with a significant positive-correlation center located in North America (Fig. 5b). The correlation pattern over the eastern North Pacific and North America is very similar to that of the positive PNA teleconnection (Wallace and Gutzler 1981), implying that during this period ENSO exerts significant influence on the atmospheric circulation of the eastern North Pacific and North America. However, there is no obvious significant correlation over East Asia, which means that the influence of ENSO on the EAWM is weak.

During 1952–76, some changes occur relative to the period of 1927–51. First, there no longer exist significant positive or negative correlations over the entire North American continent, and the significant negative-correlation center over Russia disappears (Fig. 5c). Additionally, the negative correlation located in the eastern North Pacific enlarges, extending from the eastern Pacific northwestwards to eastern Siberia. The most important change to note is registered in East Asia. Relative to the previous period, a significant positive correlation covers south China, the Korean Peninsula, and south Japan: the region where the East Asian trough is generally located (Sun and Li 1997; Wang et al. 2009). Therefore, it is suggested that during this period, ENSO might be closely related to the EAWM. Based on the above analysis, we can determine that the main impact of ENSO on the midlatitude atmospheric circulation shifts from east to west, leading to the strengthening of the ENSO–EAWM relationship.

The situation during 1977–2001 is similar to that during 1927–51. Significant positive and negative correlations are mainly located in the eastern North Pacific and North America, and the significant in-phase relationship between ENSO and East Asian circulation seems to break down during 1977–2001 (Fig. 5d). Therefore, the influence of ENSO on the midlatitude atmospheric circulation appears to shift from west back to east, leading to the weakening of the ENSO–EAWM relationship. The correlations distribution in 1902–26 (Fig. 5a) is similar to that in 1952–76 in East Asia, eastern Russia, and the North Pacific. The positive values over south Japan are not so significant as those in 1952–76 but still more significant than those in 1927–51 and 1977–2001, indicating a close relationship between ENSO and the East Asian trough, which is consistent with the results in Fig. 3a. Besides, significant positive correlations are still observed in North America, indicating a close correlation between ENSO and the PNA, which is consistent with the results in Fig. 4a.

To validate further the oscillation of the ENSO–EAWM relationship, we show the regression patterns of SLP

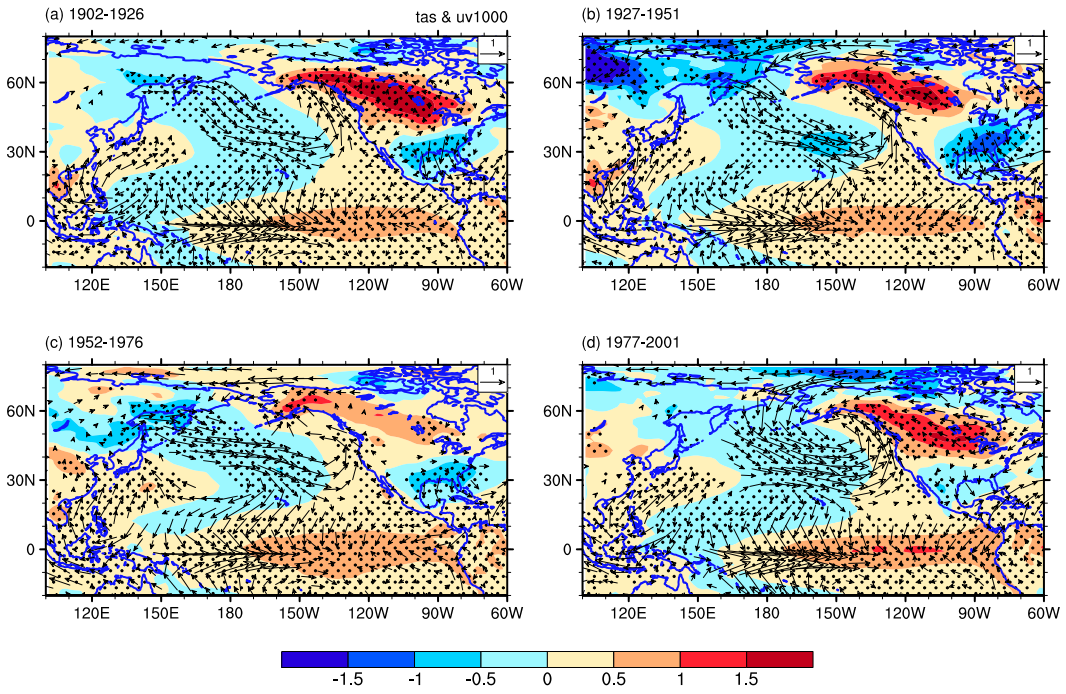

FIG. 7. As in Fig. 6, but for the 1000-hPa winds (vectors) and surface air temperature (shaded) anomalies. The surface air temperature is enclosed by dotted regions, and the vector wind are significant at the 90% confidence level based on a two-tailed Student's *t* test.

(Fig. 6), 1000-hPa wind, and SAT (Fig. 7) anomalies with respect to the Niño-3.4 index for the periods 1902–26, 1927–51, 1952–76, and 1977–2001. As can be seen, the ENSO-related midlatitude circulation anomalies exhibit remarkable differences among the four subperiods.

First, we focus on the regression pattern during 1902–26 and 1952–76 when ENSO and EAWM are highly related. In the SLP field, a positive anomaly center covers the area of the entire western Pacific and poleward to Japan (Figs. 6a,c). Meanwhile, significant negative anomalies occupy the eastern tropical and subtropical Pacific and the Bering Sea, extending westward to northern Siberia. The pattern of positive–negative anomalies oriented north–south from the low to high latitudes over the North Pacific (Figs. 6a,c) looks similar to that of the NPO (Wallace and Gutzler 1981). At 1000 hPa, an anomalous anticyclone appears in the western North Pacific and an anomalous cyclone is observed over the Bering Sea (Figs. 7a,c, vectors). The anomalous anticyclone is composed of two separate centers. One is found over the Philippine Sea and is well within the tropics. The other center is located at 30°N, 170°E, causing significant southerly wind anomalies to occur in East Asia (including southern and northern China, the Korean Peninsula, and Japan), which favors a weaker than normal EAWM. At the surface, the SAT in 1952–76 (Fig. 7c, shaded) exhibits significant positive anomalies in eastern China, the Korean Peninsula, Japan, and adjacent oceans, while significant negative anomalies are found in the Sea of Okhotsk and the high latitudes of the North Pacific. Such circulation anomalies, induced by ENSO over East Asia (Figs. 6a,c, 7a,c), are the conventional understanding of the ENSO–EAWM relationship, which has been revealed by numerous previous studies (Li 1990; Chen et al. 2000; Chang et al. 2006); warm (cold) ENSO events are concurrent with weak (strong) northerly winds along coastal East Asia and a warm (cold) East Asian continent and surrounding oceans.

The regression patterns during 1927–51 and 1977–2001 are similar to each other but with some differences to those during 1902–26 and 1952–76. In the SLP field, the NPO-like regression pattern over the North Pacific disappears, even though positive and negative anomalies still exist from the low to high latitudes, which are oriented northeast–southwest instead. (Figs. 6b,d). The regions with significant positive anomalies in the western Pacific show an obvious retreat, mainly confined to the south of 25°N. In addition, there are no longer significant negative anomalies over north Siberia and the west Bering Sea. In contrast, the negative anomalies over the northeast Pacific show a remarkable expansion and the values become greater; the negative anomaly center shifts southeastwards to the southeast of the Aleutian Islands. The striking differences in the spatial

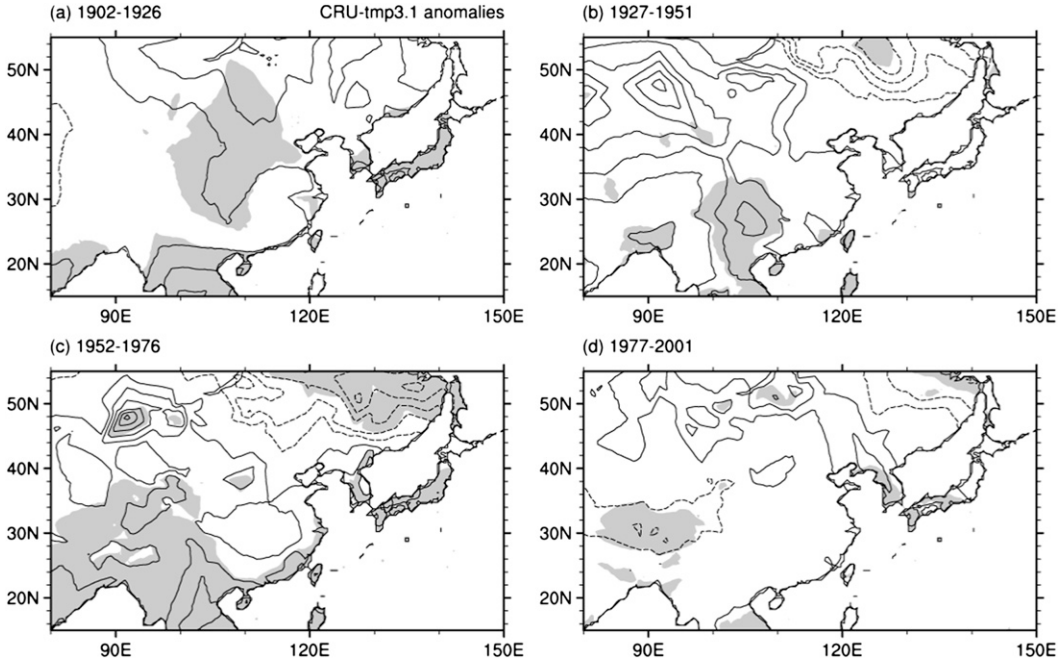

FIG. 8. Regression maps of winter near-surface temperature (CRU TS3.1) anomalies with respect to the winter Niño-3.4 index for (a) 1902–26, (b) 1927–51, (c) 1952–76, and (d) 1977–2001. The contour interval is 0.3°C and shaded values are significant at the 90% level from a two-tailed Student's *t* test.

distribution during 1927–51 and 1977–2001 from that during 1902–26 and 1952–76 suggest a strengthening relationship between ENSO and the Aleutian low, which is consistent with the results in Fig. 4 and partially revealed by He et al. (2013). At 1000 hPa, the anomalous anticyclone over the western North Pacific is much weaker during 1927–51 and 1977–2001 than during 1902–26 and 1952–76, and there is only one anomalous anticyclone center located in the Philippine Sea (Figs. 7b,d, vectors). Thus, southerly wind anomalies occur only over coastal south China, the South China Sea, and the East China Sea, mainly to the south of 30°N, and barely invade the hinterland of East Asia. Such features, so distinct from those during 1902–26 and 1952–76, indicate the weakening relationship between ENSO and the EAWM during 1927–51 and 1977–2001. At the same time, the SAT anomalies also show some distinctions, especially over East Asia and the adjacent oceans (Figs. 7b,d, shaded). The significant positive anomalies in East Asia move southward, occupying a narrower region and exhibiting smaller values than during 1952–76. Another difference of note in the midlatitudes is the enlarged significant positive anomaly in east Canada. The changes in those two regions provide other evidence to support the fact that the impact of ENSO on the East Asian winter climate is weaker and its influence on the North American winter climate is stronger during 1927–51 and 1977–2001 relative to during 1952–76.

However, the distribution of SAT anomalies seems not so convincing, especially during 1902–26 when the atmospheric circulation anomalies over East Asia are more significant than those during 1927–51, while the SAT anomalies are exceptions. We suggest those results are comprehensible and acceptable because the ENSO–EAWM relationship is barely significant at the 95% confidence level during 1902–26 (Fig. 3a). In addition, the reanalysis data errors might be an important factor. Therefore, we repeat the temperature anomalies related to ENSO using the observational near-surface temperature anomalies derived from CRU TS3.1 (Fig. 8). Interestingly, the temperature anomalies over East Asia during 1902–26 (Fig. 8a) and 1952–76 (Fig. 8c) are obviously more significant than those during 1927–51 (Fig. 8b) and 1977–2001 (Fig. 8d), respectively, especially in Japan, which well supports the atmospheric circulation anomalies derived from the NOAA reanalysis datasets.

4. Possible mechanisms for the change in the ENSO–EAWM relationship

The contrast in the relationship between ENSO and the midlatitude circulation anomalies in the four subperiods confirms the inconsistent impact of ENSO on the East Asian winter monsoon and raises two questions. First, why is the ENSO–EAWM relationship weakened or strengthened at certain times? Second, why does the

ENSO–EAWM relationship take on a quasi-50-yr oscillation? In this section, we try to answer these two questions.

a. Weakening and southeastward shift in the Walker circulation

To address the first question, a good understanding of the mechanism by which ENSO affects the East Asian monsoon is required. In the conventional description, the Walker circulation is thought to provide a mechanism connecting ENSO and monsoon. It is characterized by westerly winds across the central Pacific in the upper troposphere, a sinking motion over the eastern Pacific, a returning flow from east to west at lower level, and a rising motion over the western Pacific (Bjerknes 1969). During an El Niño event, the rising limb of the Walker circulation in the western Pacific shifts eastward to the central and eastern Pacific. Therefore, an anomalous subsidence is induced over the western Pacific, East Asia, and the Indian subcontinent. Consequently, there is an anomalously high pressure over the western Pacific because the anomalous subsidence suppresses convection in this region. This is associated with an anomalous anticyclone in the low-level troposphere over the western Pacific (Figs. 6 and 7). In other words, the intensity and location of the anomalous anticyclone in the western Pacific relies heavily on the intensity and location of anomalous subsidence induced by the Walker circulation in this region.

However, a southeastward shift and weakening trend in the Walker circulation during the twentieth century have been noted by Tanaka et al. (2004) and simulated by most models used for the Intergovernmental Panel on Climate Change Fourth Assessment Report (Cai et al. 2010). During the El Niño events of 1958–80, the anomalous subsidence motion is mainly located over the East Asian continent; whereas during 1981–99, a significant southeastward shift is observed in the Walker circulation, and the center of anomalous subsidence almost moves out of East Asia (see Kumar et al. 1999, their Fig. 2). In the present study, we also observe a similar change. The anomalously high pressure in the western Pacific during 1952–76 (Fig. 6c) is located farther north than during 1977–2001 (Fig. 6d). Therefore, the southeastward shift of the Walker circulation in the late 1970s might be one of the main reasons why the anomalous anticyclone covers the entire western Pacific during 1952–76 (Fig. 7c), while it only extends over the Philippine Sea during 1977–2001 (Fig. 7d).

Can the changes identified above in the ENSO-related circulation anomalies before the 1950s be explained from the perspective of the Walker circulation? To answer this question, we calculate El Niño year composites of velocity potential anomalies at both 200 and 850 hPa during 1902–26 and 1927–51. The composites, corresponding to the El Niño events of 1902–26 (Fig. 9a), exhibit significant anomalous subsidence motion (positive values) over the Indian Ocean, East Asia, and western Pacific, and anomalous rising motion (negative values) in the eastern Pacific and North America. The center of anomalous subsidence motion is located in the western Pacific, north of the equator. By contrast, the composites of El Niño events during 1927–51 (Fig. 9c) show an obvious southeastward shift in the center of anomalous subsidence motion. The significant anomalous positive values are located over the Philippine Sea and northwest Australia. Similar results, but with an opposite sign, are obtained from the composites of anomalies at 850 hPa (Figs. 9b,d).

We gave further the regression maps of 300-hPa divergence and divergent wind components' anomalies with respect to the winter Niño-3.4 index for the four subperiods in Fig. 10. And the most striking distinction is located in the western Pacific and East Asia. The convergence over the western Pacific during 1902–26 (Fig. 10a) is more significant than that during 1927–51 (Fig. 10b). While the divergence over East Asia during 1952–76 (Fig. 10c) is more significant than that during 1977–2001 (Fig. 10d). That means the low troposphere southerly wind anomalies induced by warm ENSO over coastal East Asia would be stronger during 1902–26 and 1952–76 than those during 1927–51 and 1977–2001, which is attributed to the interdecadal change of the Walker circulation. What is more, in the long term, the positive (negative) phase of the Walker circulation index (figure is not shown) is well concurrent with the strong (weak) ENSO–EAWM relationship.

The above fundamental mechanism emphasizes the modulation of the Walker circulation on the intensity and location of the anomalous anticyclone in the western Pacific (hereafter referred to as WPAC). In fact, the important role of the WPAC in bridging the warming in the eastern central Pacific and weak East Asian winter monsoon through a PEAT confined to the lower troposphere has been noticed by Wang et al. (2000). They highlighted that the WPAC contains two separate centers: one located over the Philippine Sea and the other at 40°N, 170°E. However, from the present study, the PEAT is not always well established. Only when the anomalous subsidence of the Walker circulation is located more northward can a pair of anomalous anticyclones be observed over the western Pacific (Figs. 7a,c). Therefore, a large area of anomalous southwesterlies prevails in East Asia and the adjacent oceans, implying a weaker EAWM. In this sense, the anomalous anticyclone located over the Kuroshio Extension, rather than the Philippine anticyclone, is a key system connecting

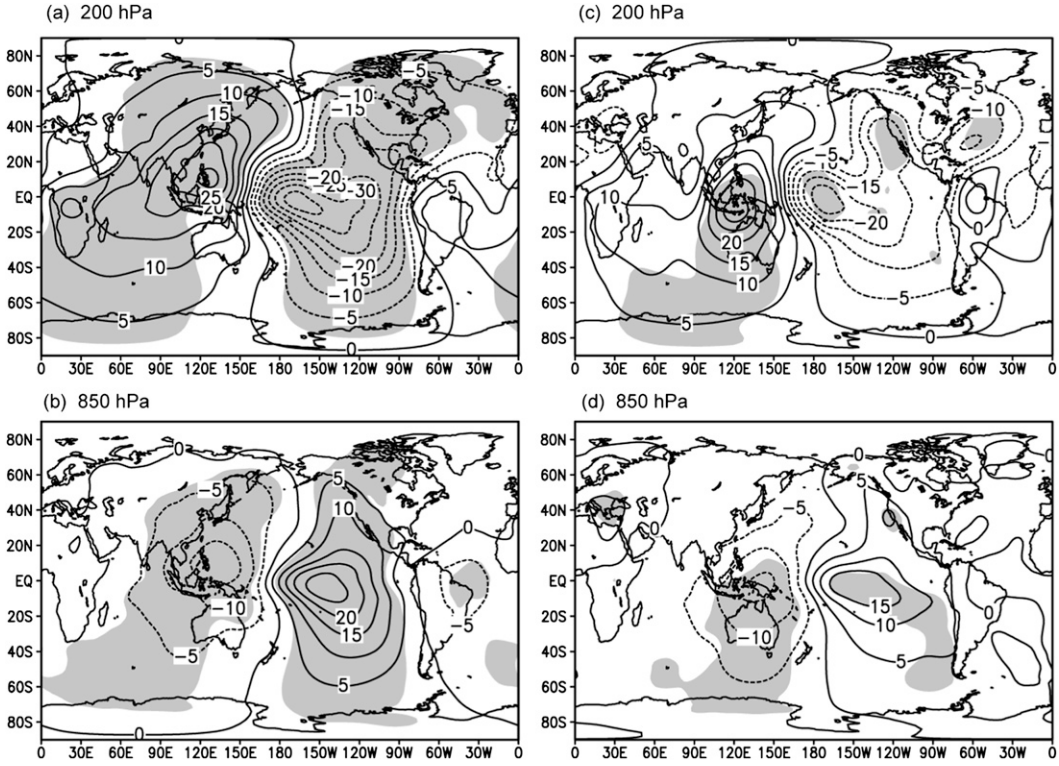

FIG. 9. Composite difference of winter velocity potential ($10^{-5}\,m^2\,s^{-1}$) during 1902–26 at (a) 200 and (b) 850 hPa and 1927–51 at (c) 200 and (d) 850 hPa for the El Niño events. The El Niño years are identified by Niño-3.4 SST anomalies during winter exceeding 0.5 standard deviation. Shaded values are significant at the 95% level from a two-tailed Student's *t* test.

ENSO and the EAWM, which is somewhat different from the viewpoint of Wang et al. (2000). To support our speculation, we further display the 23-yr sliding correlation of the Niño-3.4 index with the area-averaged SLP anomalies over the Philippine Sea (PHS; 10°–20°N, 120°–150°E) and northwestern Pacific basin (NWP; 22°–50°N, 140°E–180°) (Fig. 11). As we can see, the relationship between ENSO and the SLP anomalies over the PHS is consistently highly correlated. In contrast, the relationship between ENSO and SLP anomalies over the NWP shows an obvious low-frequency oscillation, and the evolution is much more concurrent with that of the ENSO–EAWM relationship, as depicted in Fig. 3. In summary, the southeastward (northwestward) shift in the Walker circulation weakens (strengthens) the impact of ENSO on the anomalous anticyclone over the NWP; thus, the ENSO–EAWM relationship is therefore weakened (strengthened).

b. Modulation of the AMO and PDO

We attempt to settle the second question by focusing on the multidecadal variation of sea surface temperature. The multidecadal variations in the North Pacific are often referred to as the PDO (Mantua et al. 1997) and those in the Atlantic Ocean are known as the AMO (Kerr 2000). WCH08 indicated that the PDO could modulate the impact of ENSO on the East Asian winter monsoon. When the PDO is in its low (high) phase, the ENSO–EAWM relationship is significant (insignificant). Such a theory is plausible for the second half of the last century (Fig. 12); however, the results prior to the 1950s conflict somewhat with the findings of WCH08. For example, the ENSO–EAWM relationship is insignificant during 1927–51, but there are both high and low PDO phases. In addition, even though the PDO is mainly in its high phase during 1900–26, there is a robust and significant relationship between ENSO and the EAWM. Therefore, the above analysis suggests that the modulation of PDO on the ENSO–EAWM relationship functions only after the 1950s. Prior to the 1950s, it seems that the evolution of the ENSO–EAWM relationship might be modulated by the AMO. The warm (cool) phase of the AMO coincides well with the insignificant (significant) ENSO–EAWM relationship (Fig. 12). Dong et al. (2006) indicated that the warm AMO is related to weaker ENSO variability. Moreover, Li and Bates (2007) revealed that the warm AMO could induce a weaker East Asian winter monsoon. Therefore, a weaker

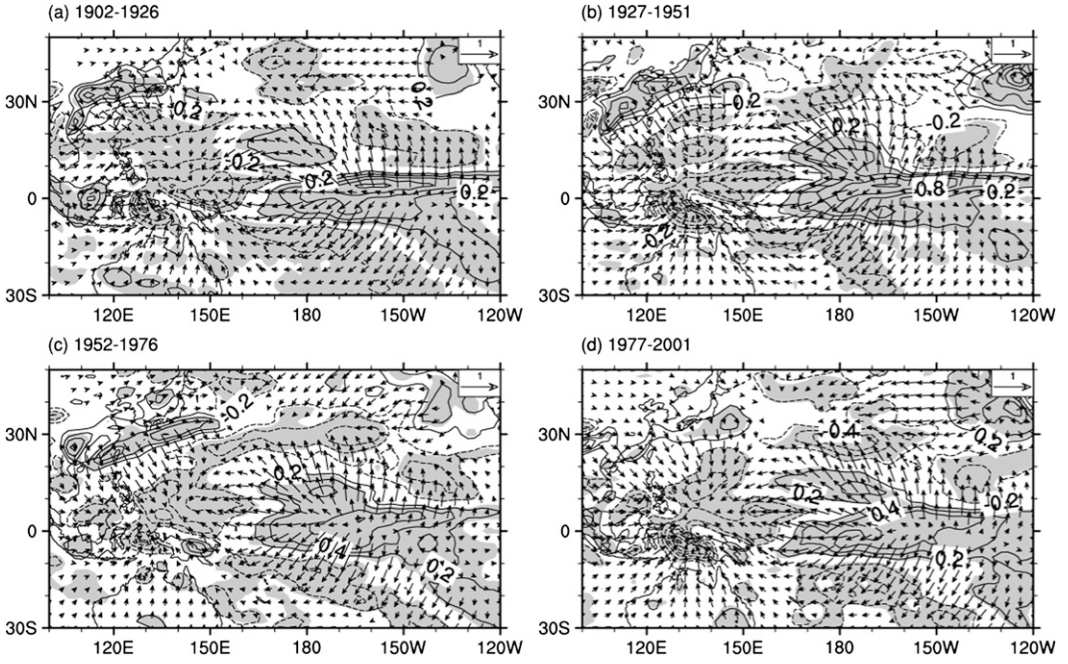

FIG. 10. Regression maps of 300-hPa divergence (contour: $10^{-6}\,s^{-1}$) and divergent wind components (vectors: $m\,s^{-1}$) anomalies with respect to the winter Niño-3.4 index for (a) 1902–26, (b) 1927–51, (c) 1952–76, and (d) 1977–2001, respectively. The divergence enclosed by shaded regions and the vector wind are significant at the 90% confidence level based on a two-tailed Student's *t* test.

ENSO–EAWM relationship is possibly associated with the warm phase of the AMO. Consequently, the low-frequency oscillation of the ENSO–EAWM relationship might be attributed to the combined effect of the PDO and AMO, which could be supported further by the temporal evolution of the AMO + PDO index (Fig. 12). Another important problem is how the PDO and AMO modulate the ENSO–EAWM relationship. Previous studies have indicated that the impact of ENSO could be transmitted to extratropical regions through the "atmospheric bridge"

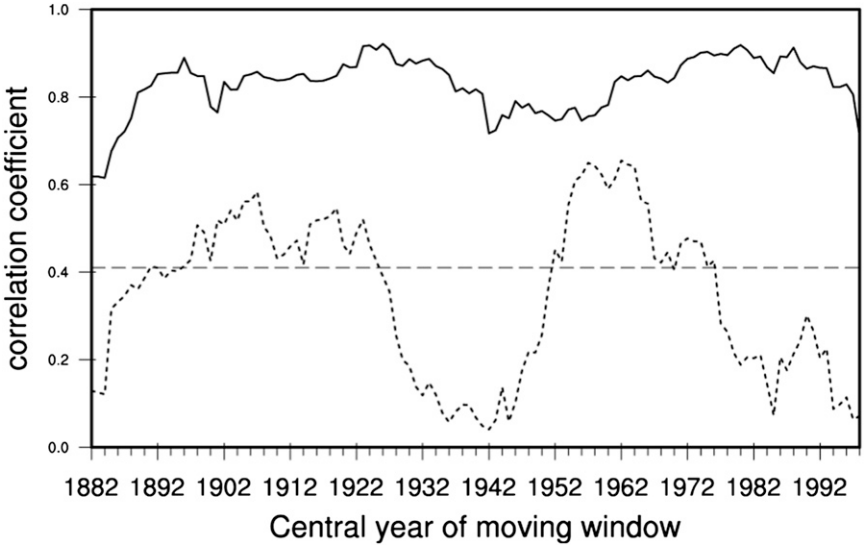

FIG. 11. The 23-yr sliding correlation of the winter Niño-3.4 index with the sea level pressure anomalies over the Philippine Sea (10°–20°N, 120°–150°E) (solid curve) and northwestern Pacific basin (22°–50°N, 140°E–180°) (dashed curve). Horizontal dashed line indicates the 95% significant level from a two-tailed Student's *t* test.

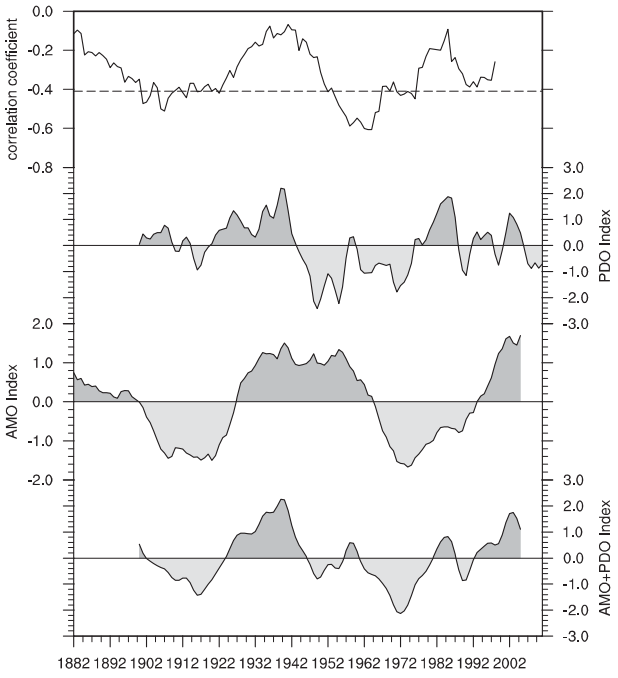

FIG. 12. The 23-yr sliding correlation of the winter Niño-3.4 index with the EAWMI (solid curve); horizontal dashed line indicates the 95% significant level. Shaded curves from top to bottom are the normalized PDO index, AMO index, and AMO + PDO index, respectively.

(Lau and Nath 1996; Lau 1997; Alexander et al. 2002), which means that the climatological background field over the North Pacific plays an important role in the interaction between ENSO and atmospheric circulation. Thus, a question to be addressed is whether the climatological background field varies with the phase of the PDO/AMO.

Figure 13 presents the regressed SLP anomalies on the winter Niño-3.4 index for different phases of the PDO (Figs. 13a,b) and AMO (Figs. 13c,d). Clearly, even though the spatial distribution of SLP anomalies is similar in the tropical regions, great distinctions appear in the mid- and high latitudes between the high and low phase of the PDO. During the high phase of the PDO (Fig. 13a), significant negative anomalies are observed over the northeastern Pacific and western Atlantic. Two negative centers are located southeast of the Aleutian Islands and near Bermuda. The regressed fields of the low phase of the PDO show a significant northwestward shift in the Aleutian low and a northeastward shift of the negative center near Bermuda (Fig. 13b). There are other significant negative anomalies over eastern Siberia, and a negative center appears northwest of the Aleutian Islands. The SLP anomalies in the low phase of the PDO imply a weakened Siberian high and an intensified NPO (Wallace and Gutzler 1981). Similar results are obtained from the regressed SLP anomalies on the Niño-3.4 index for different phases of the AMO (Figs. 13c,d). Note that the spatial distribution of SLP anomalies in the high (Figs. 13a,c) and low (Figs. 13b,d) phase of the PDO/AMO is quite similar to that during periods of weak (Figs. 6b,d) and strong (Figs. 6a,c) ENSO–EAWM relationship. This implies that the low phase of the PDO/AMO might be beneficial to the establishment of the positive NPO, favoring a weaker than normal EAWM during El Niño years. It should be noted that the SLP anomalies over the Bering Sea during the low phase of the PDO/AMO resemble the one-point correlations of SLP anomalies based on 65°N, 170°E (see Linkin and Nigam 2008, their Fig. 1b). Thus, the correlation between ENSO and SLP anomalies over the Bering Sea is significant (insignificant) during the low (high) phase of the PDO/AMO, implying a strengthening (weakening) of the ENSO–NPO relationship. As a result, ENSO exerts strong (weak) influence on the EAWM.

To illustrate the important role of SLP anomalies over the Bering Sea in connecting ENSO to the EAWM, Fig. 14 presents the 23-yr sliding correlation between the Niño-3.4 index and the area-averaged SLP anomalies over the north Bering Sea (60°–70°N, 140E°–180°). A clear low-frequency oscillation is obtained and the time evolution is similar to that of the ENSO–EAWM relationship (Fig. 3, solid curve), which further supports the aforementioned conjecture.

5. Recent recovery of the ENSO–EAWM relationship?

Using the 23-yr sliding correlation to determine the exact relationship between ENSO and the EAWM for the present data up to 2024 is required, but these data are currently unavailable. However, we suggest that the above analysis might provide three lines of supporting evidence for the current ENSO–EAWM relationship. As discussed above, the ENSO–EAWM relationship undergoes a low-frequency oscillation with a period of about 50 yr. From Figs. 3, 11, and 14 we can establish that the last century saw two full oscillating cycles. One is 1902–51, which consists of a strong (1902–26) and a weak (1927–51) ENSO–EAWM relationship. During 1952–76, the ENSO–EAWM relationship returns to a significantly closer relationship but subsequently enters into its weak correlation period (1977–2001). Therefore, another period with a strong ENSO–EAWM relationship is likely coming. On the other hand, as indicated in section 4, it is the PDO that modulates the ENSO–EAWM relationship after the 1950s; this is somewhat consistent with the results of WCH08. Meanwhile, it seems that the PDO entered into its negative phase in the

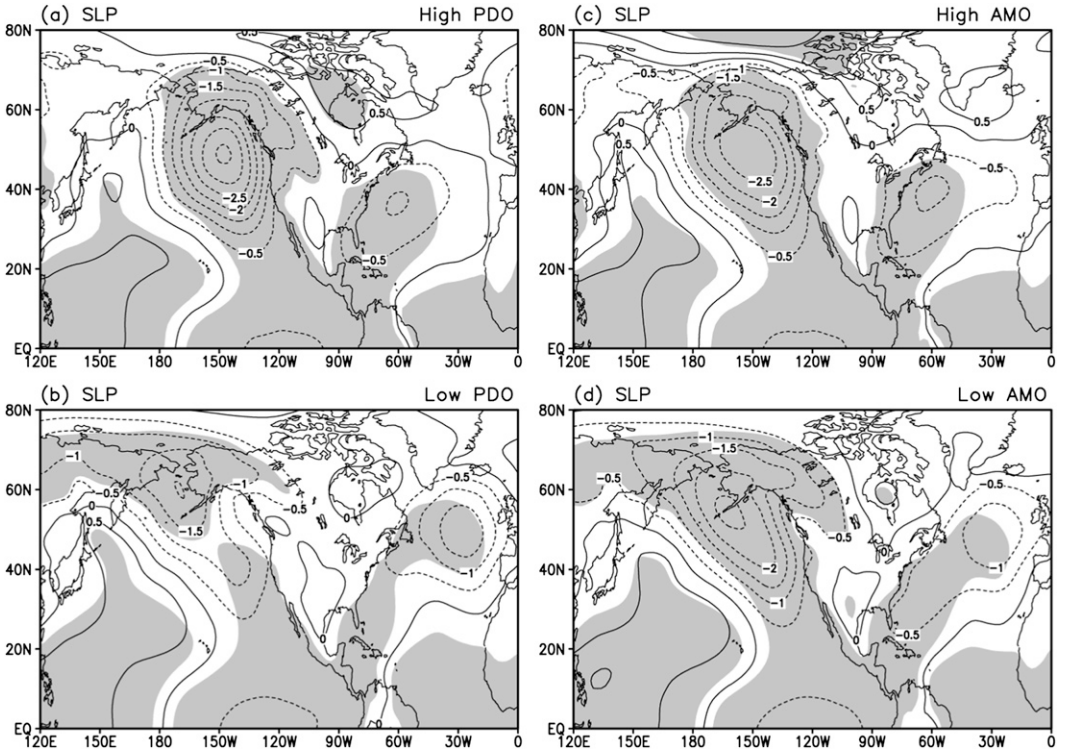

FIG. 13. Regression maps for the winter SLP with respect to winter Niño-3.4 index in (a),(c) high and (b),(d) low phase of the PDO/AMO during the period 1900–2005. Shaded values are significant at the 95% level from a two-tailed Student's *t* test.

early 2000s (Fig. 12), which has been suggested by Lee and McPhaden (2008) and confirmed by Cai and van Rensch (2012). Therefore, the transition of the PDO to its negative phase constitutes the second line of evidence supporting a switch in the ENSO–EAWM relationship to a significant status. In addition, the above analysis indicates that stronger Walker circulation might be favorable for a stronger ENSO–EAWM relationship. So the third line

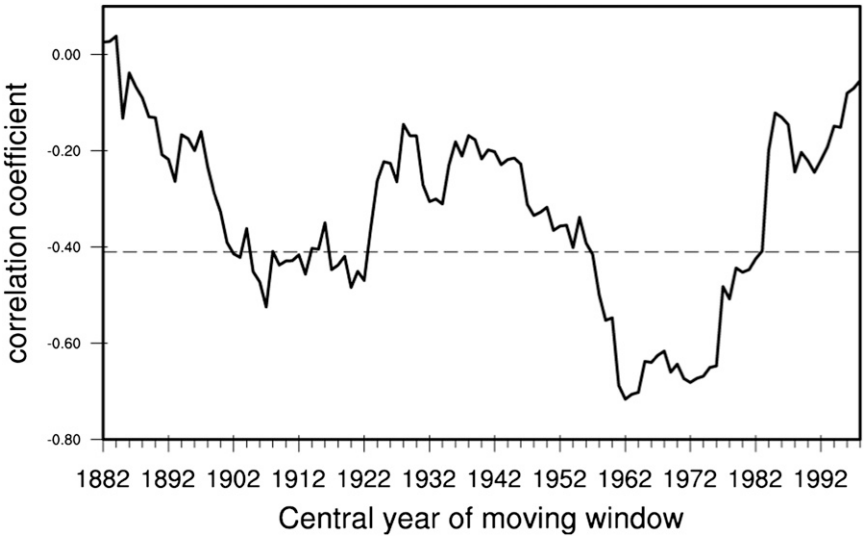

FIG. 14. The 23-yr sliding correlation of the winter Niño-3.4 index with the SLP anomalies over the north Bering Sea (60°–70°N, 140°E–180°). Horizontal dashed line indicates the 95% significant level from a two-tailed Student's *t* test.

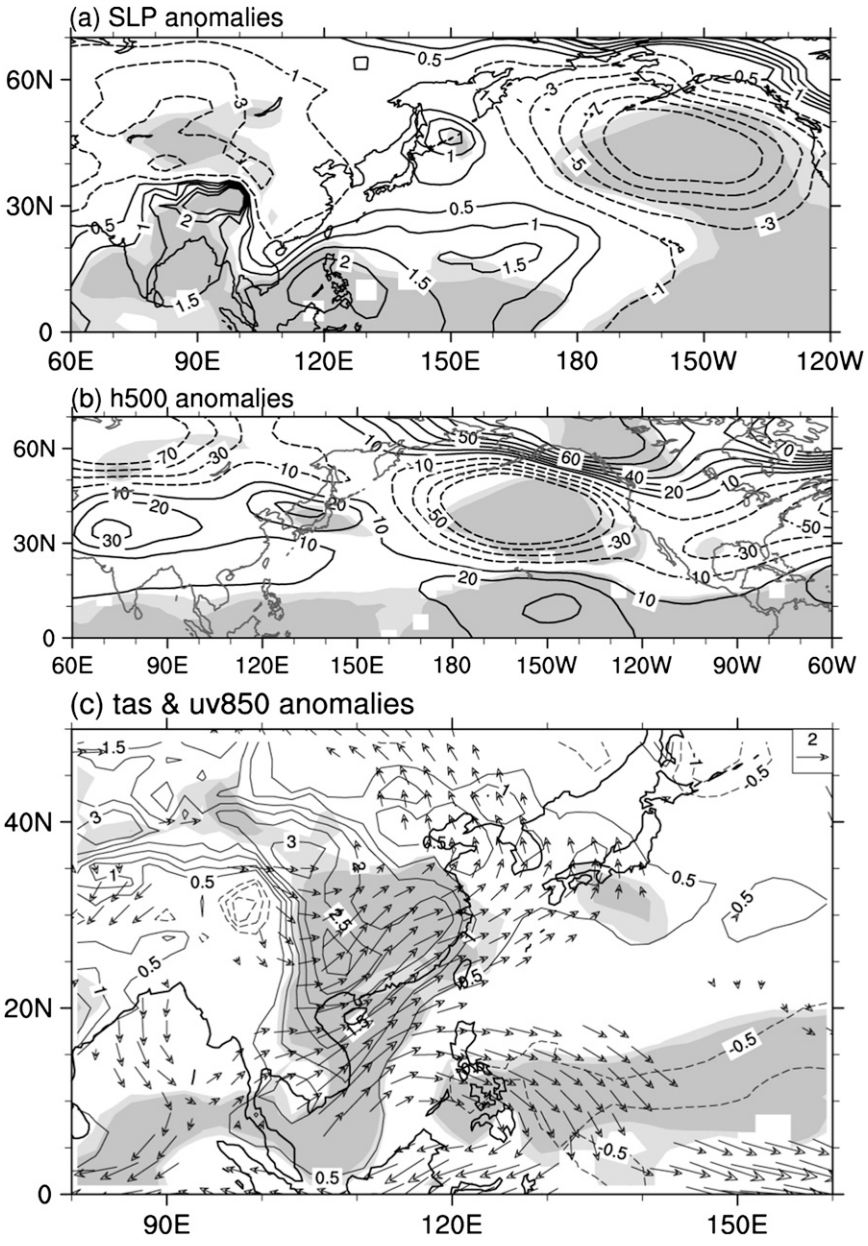

FIG. 15. Composite difference of winter (a) sea level pressure, (b) 500-hPa geopotential height, and (c) surface air temperature at 2 m (contours) and 850-hPa wind (vectors) anomalies between El Niño events (years of 2002 and 2009) and La Niña events (years of 2005, 2007, 2010, and 2011). Light and dark shaded values are significant at the 90% and 95% (vector for 90%) significant levels from a two-tailed Student's *t* test, respectively.

of evidence comes from the enhancement of the Walker circulation in the late 1990s (Dong and Lu 2013).

To examine the recent strengthening in the connection between ENSO and the EAWM, we gave further the composites of SLP, H500, and SAT anomalies between El Niño events and La Niña events during 2002–12. The composites indicate that corresponding to El Niño events, significant negative SLP anomalies come up in Siberia and significant positive ones are observed in the western Pacific (Fig. 15a), suggesting a weakened Siberian high and a strengthened western Pacific anticyclone. At the same time, the East Asian trough is weakened (Fig. 15b) and there is extensive anomalous southerly wind; significant positive SAT anomalies emerge in East Asia (Fig. 15c). Therefore, it is suggested that ENSO has recently entered into its period of strong influence on the EAWM.

6. Summary and concluding remarks

Based on the Twentieth Century Reanalysis, version 2, datasets, we investigated the interdecadal variations in the relationship between ENSO and the East Asian winter monsoon during the last century. The 23-yr sliding correlation between the Niño-3.4 index and the EAWM index indicates that a low-frequency oscillation with a period of about 50 yr might exist in the ENSO–EAWM relationship (Fig. 3). This means that periods of a significant ENSO–EAWM relationship alternate with periods when it is insignificant during the winters throughout the entire period of 1871–2009. Specifically, the ENSO–EAWM relationship is consistently highly correlated during 1902–26 and 1952–56 but appears to break down during 1927–51 and 1977–2001. Hereafter, we call a high-correlation period (HCP) and a low-correlation period (LCP). We compared the correlation of the winter Niño-3.4 index with the 500-hPa geopotential height anomalies between the HCPs and LCPs (Fig. 5). The spatial distribution of the correlations shows a pronounced distinction over East Asia, the North Pacific, and North America for different periods. In HCPs, significant positive correlations are observed in the East Asian trough, and significant negative correlations are located in eastern Siberia, the Bering Sea, and the northeastern Pacific. The ''positive–negative'' anomalies oriented north–south from low latitudes to high latitudes in the North Pacific are very similar to the positive NPO, which is supported by the temporal evolution of the 23-yr sliding correlation between the Niño-3.4 index and NPO index (Fig. 3). This implies that ENSO exerts strong influence on the EAWM in HCPs, but in LCPs, the NPO-like correlation pattern disappears. In contrast, significant negative and positive correlations oriented northeast–southwest appear in the eastern North Pacific and North America, respectively. This indicates that the impact of ENSO shifts eastward, leading to a weakening of the ENSO–EAWM relationship. The climatic changes identified above can also be clearly depicted by the regression patterns of SLP, the 1000-hPa wind, and SAT anomalies with respect to the Niño-3.4 index in HCPs and LCPs (Figs. 6, 7, 8). Corresponding to the warm ENSO events in HCPs, there is a significant positive SLP anomaly center covering the area of the entire western Pacific and poleward to Japan. This is accompanied by significant negative anomalies occupying the eastern tropical and subtropical Pacific and the Bering Sea, extending westward to northern Siberia. Consistent with the anomalies in the SLP field, there is an obvious anomalous anticyclone in the western Pacific and a significant anomalous cyclone over the Bering Sea. The anomalous anticyclone contains two separate centers, which are located over the Philippine Sea and Kuroshio Extension (around 30°N, 170°E). The anomalous anticyclone center (30°N, 170°E), which is beneficial for the establishment of the PEAT (Wang et al. 2000; WCH08), leads to strong and significant southerly winds penetrating to 50°N along coastal East Asia. Therefore, ENSO exerts a strong impact on the EAWM, for which further evidence is provided by the significant positive anomalies of SAT over south China, east China, and the adjacent oceans. In contrast, the regression patterns in LCPs show great differences from those in HCPs. First, the significant positive SLP anomalies retreat southward and become mainly confined to the area south of 25°N. At the same time, the significant negative SLP anomaly center located in the Bering Sea shifts southeastwards to the southeast of the Aleutian Islands. Second, the anomalous anticyclone center at 30°N, 170°E disappears with only the Philippine anomalous anticyclone remaining. This suggests that the PEAT is not well established and that the EAWM can hardly be influenced by ENSO. Third, almost no significant positive SAT anomalies are observed in the East Asian continent and their values and extent in the adjacent oceans become smaller, which gives direct evidence of a weakened ENSO–EAWM relationship.

The Walker circulation is thought to be an important means by which ENSO influences the monsoon. It is indicated that significant anomalous subsidence of the Walker circulation, corresponding to El Niño events in HCPs, is found over the Indian Ocean, the East Asian continent, and the western Pacific (Figs. 9, 10). The center of anomalous subsidence motion is located in the western Pacific, north of equator. As a result, the convection in this region is suppressed and an anomalously high pressure is induced, which could extend to the north of 45°N, leading to an anomalous anticyclone with two separate centers covering the entire western Pacific. This implies that the PEAT is well established and that ENSO can exert a strong influence on the EAWM. However, the Walker circulation features notable distinctions in LCPs. The most striking change is the obvious southeastward shift in the center of the anomalous subsidence motions, which is mainly confined to the Philippine Sea and northwestern Australia. Consequently, the anomalous high pressure retreats southward to the north of 20°N, and there is only one anomalous anticyclone observed in the Philippine Sea. The associated southerly wind along coastal East Asia is insignificant and can hardly penetrate into the East Asian continent; in other words, the ENSO–EAWM relationship is relatively weak. The above fundamental mechanism emphasizes the modulation of the Walker circulation on the intensity of the anomalous anticyclone located around

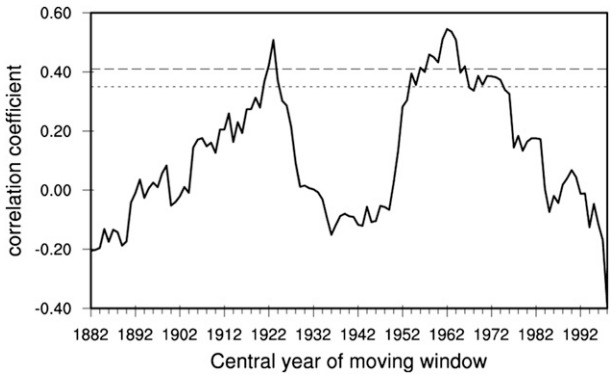

FIG. 16. The 23-yr sliding correlation between the winter Niño-3.4 index and NPOI defined as the HadSLP2r. The short and long horizontal dashed lines indicate the 90% and 95% significant levels, respectively.

30°N, 170°E, which we suggest is the key system bridging ENSO and the EAWM. Such a viewpoint is supported further by the 23-yr sliding correlation between the Niño-3.4 index and the area-averaged SLP anomalies in the region of 22°–50°N and 140°E–180° (Fig. 11), the temporal evolution of which also shows a clear quasi-50-yr low-frequency oscillation.

One cause for the quasi-50-yr low-frequency oscillation in the ENSO–EAWM relationship might be the modulation of the PDO and the AMO. Comparing the temporal evolution of the ENSO–EAWM relationship with those of the PDO index and AMO index, we find that the low (high) phase of the PDO is well concurrent with the high (low) ENSO–EAWM relationship during 1952–2001, and the high (low) ENSO–EAWM relationship generally shows up in the low (high) phase of the AMO during 1882–1951 (Fig. 12). Therefore, we suggest that the combined effect of the PDO and AMO might contribute to the low-frequency oscillation of the ENSO–EAWM relationship, which can be supported further by the temporal evolution of the AMO + PDO index. The way in which the PDO/AMO influences the ENSO–EAWM relationship is through its impact on the SLP anomalies around 65°N, 170°E, which is one of the base points for the definition of the NPO (Wallace and Gutzler 1981) (Fig. 13). More evidence emerges from the quasi-50-yr low-frequency oscillation in the relationship between the Niño-3.4 index and the area-averaged SLP anomalies in the domain of 60°–70°N and 140°E–180°(Fig. 14).

Given that the ENSO–EAWM relationship has experienced about two full oscillating cycles (1902–51 and 1952–2001) and in recent decades has mainly been modulated by the PDO, which might have entered its low phase in the 2000s (Cai and van Rensch 2012) as well as the enhancement of Walker circulation in the late 1990s (Dong and Lu 2013), we suggest that ENSO and the EAWM might be closely correlated at present. The preliminary supporting evidence for this speculation comes from the composites of EAWM-related climate anomalies between El Niño events and La Niña events during 2002–12 (Fig. 15). Corresponding to warm ENSO events, significant negative and positive SLP anomalies are observed in Siberia and the western Pacific, respectively, suggesting a weakened west–east SLP gradient.

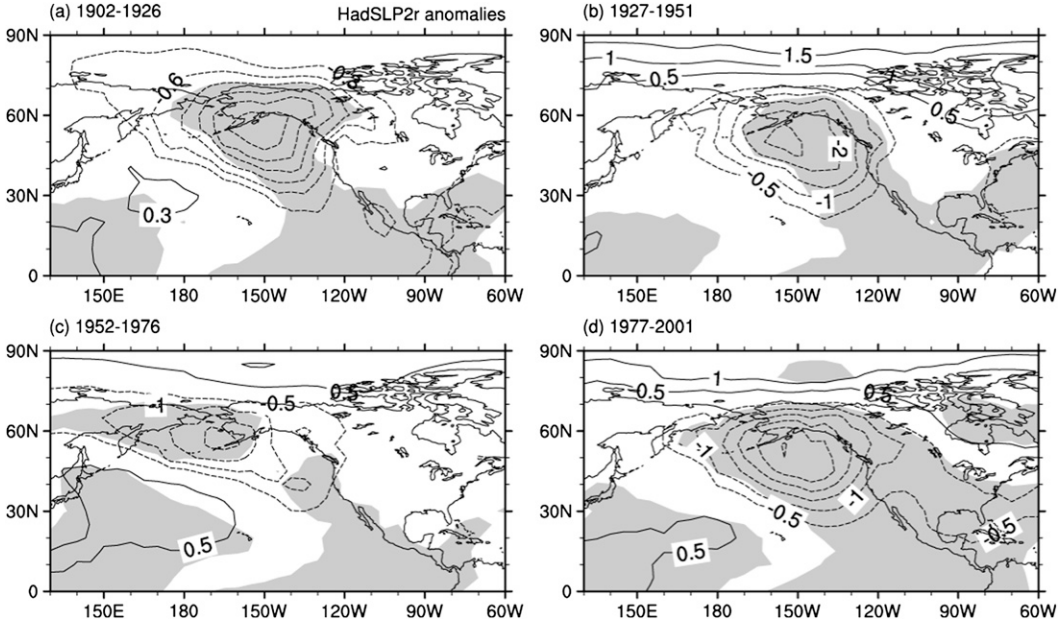

FIG. 17. As in Fig. 6, but for the HadSLP2r.

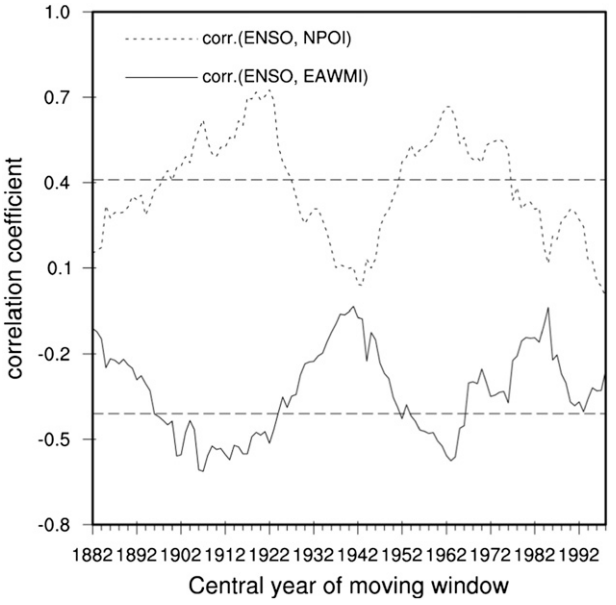

FIG. 18. The 23-yr sliding correlation between the autumn Niño-3.4 index and EAWMI (solid curve) and winter NPOI (dashed curve). The horizontal dashed lines indicates the 95% significant level.

At the same time, the East Asian trough is weakened and extensive anomalous southerly wind prevails in East Asia. Correspondingly, significant positive SAT anomalies emerge in East Asia. Therefore, it is suggested that ENSO has recently entered into its period of strong influence on the EAWM.

The mechanism responsible for the low-frequency oscillation of the ENSO–EAWM relationship is rather complex. In addition to the PDO, AMO, and Walker circulation discussed above, other external factors (e.g., snow cover and sunspot) may exert impact on the EAWM variability through feedback processes with ENSO (Zhou et al. 2007a,b). On the other hand, EAWM and ENSO are characterized by internal variability. A remarkable reduction is found in the interannual variability of EAWM (He 2013). Meanwhile, the blocking variability over the Ural Mountain region in boreal winter changes a lot (Zhou et al. 2009; Cheung et al. 2013), and the impact of Ural blocking on the East Asian winter climate also shows instability (Wang et al. 2010; Cheung et al. 2012). The warm ENSO episode becomes more frequent since the mid-1970s (Lau and Nath 1996). This is consistent with the Southern Oscillation index trends that show negative values since the late 1970s (Namias et al. 1988; Nitta and Yamada 1989). To what extent the internal variable of ENSO and EAWM contributes to the unstable ENSO–EAWM relationship is still an open question. Besides, most of the analysis above is based on the NOAA reanalysis datasets. Are the results reliable? We turn to the observational datasets to address this question. Figure 16 displays the 23-yr sliding correlation between the Niño-3.4 index and North Pacific Oscillation index (NPOI) defined as the HadSLP2r. Even though it is a little different from the results derived from the NOAA reanalysis (Fig. 3), an obvious low-frequency oscillation is still observed. What is more, the observed SLP anomalies related to ENSO (Fig. 17) are much similar to the reanalysis results (Fig. 6). And the observed temperature anomalies related to ENSO derived from CRU TS3.1 (Fig. 8) also support the results obtained from the NOAA reanalysis datasets. Therefore, low-frequency oscillation exists very likely in the ENSO–EAWM relationship. The time–lag relationship emphasizes the possible forcing of ENSO on the EAWM (Fig. 18); however, to better understand the physical processes of the unstable ENSO–EAWM relationship, more work and modeling studies are needed.

Acknowledgments. This research was supported by the National Natural Science foundation of China under Grants 41130103 and 41210007.

REFERENCES

Alexander, M. A., I. Bladé, M. Newman, J. R. Lanzante, N.-C. Lau, and J. D. Scott, 2002: The atmospheric bridge: The influence of ENSO teleconnections on air–sea interaction over the global oceans. *J. Climate,* **15,** 2205–2231.

Allan, R. J., and T. J. Ansell, 2006: A new globally complete monthly historical mean sea level pressure data set (HadSLP2): 1850–2004. *J. Climate,* **19,** 5816–5842.

Bjerknes, J., 1969: Atmospheric teleconnections from the equatorial Pacific. *Mon. Wea. Rev.,* **97,** 163–172.

Boyle, J. S., and T. J. Chen, 1987: Synoptic aspects of the wintertime East Asian monsoon. *Monsoon Meteorology,* C. P. Chang and T. N. Krishnamurti, Eds., Oxford University Press, 125–160.

Cai, W., and P. van Rensch, 2012: The 2011 southeast Queensland extreme summer rainfall: A confirmation of a negative Pacific decadal oscillation phase? *Geophys. Res. Lett.,* **39,** L08702, doi:10.1029/2011GL050820.

——, ——, T. Cowan, and A. Sullivan, 2010: Asymmetry in ENSO teleconnection with regional rainfall, its multidecadal variability, and impact. *J. Climate,* **23,** 4944–4955.

Chang, C. P., and K. M. Lau, 1982: Short-term planetary-scale interactions over the tropics and midlatitudes during northern winter. Part I: Contrasts between active and inactive periods. *Mon. Wea. Rev.,* **110,** 933–946.

——, Z. Wang, and H. Hendon, 2006: The Asian winter monsoon. *The Asian Monsoon,* B. Wang, Ed., Springer, 89–127.

Chen, W., and R. H. Huang, 2002: The propagation and transport effect of planetary waves in the Northern Hemisphere winter. *Adv. Atmos. Sci.,* **19,** 1113–1126.

——, H. F. Graf, and R. Huang, 2000: The interannual variability of East Asian winter monsoon and its relation to the summer monsoon. *Adv. Atmos. Sci.,* **17,** 48–60.

——, S. Yang, and R. H. Huang, 2005: Relationship between stationary planetary wave activity and the East Asian winter monsoon. *J. Geophys. Res.,* **110,** D14110, doi:10.1029/2004JD005669.

Cheng, Y., Y. Tang, and D. Chen, 2011: Relationship between predictability and forecast skill of ENSO on various time scales. *J. Geophys. Res.,* **116,** C12006, doi:10.1029/2011JC007249.

Cheung, H., W. Zhou, H. Mok, and M. Wu, 2012: Relationship between Ural–Siberian blocking and the East Asian winter monsoon in relation to the Arctic Oscillation and the El Niño–Southern Oscillation? *J. Climate,* **25,** 4242–4257.

——, ——, ——, ——, and Y. Shao, 2013: Revisiting the climatology of atmospheric blocking in the Northern Hemisphere? *Adv. Atmos. Sci.,* **30,** 397–410.

Compo, G., and Coauthors, 2011: The Twentieth Century Reanalysis Project. *Quart. J. Roy. Meteor. Soc.,* **137,** 1–28.

Deser, C., M. A. Alexander, and M. S. Timlin, 1996: Upper-ocean thermal variations in the North Pacific during 1970–1991. *J. Climate,* **9,** 1840–1855.

Ding, Y., and T. N. Krishnamurti, 1987: Heat budget of the Siberian high and the winter monsoon. *Mon. Wea. Rev.,* **115,** 2428–2449.

Dong, B., and R. Lu, 2013: Interdecadal enhancement of the Walker circulation over the tropical Pacific in the late 1990s. *Adv. Atmos. Sci.,* **30,** 247–262.

——, R. T. Sutton, and A. A. Scaife, 2006: Multidecadal modulation of El Niño–Southern Oscillation (ENSO) variance by Atlantic Ocean sea surface temperatures. *Geophys. Res. Lett.,* **33,** L08705, doi:10.1029/2006GL025766.

Gollan, G., R. J. Greatbatch, and T. Jung, 2012: Tropical impact on the East Asian winter monsoon. *Geophys. Res. Lett.,* **39,** L17801, doi:10.1029/2012GL052978.

Gong, D. Y., S. W. Wang, and J. H. Zhu, 2001: East Asian winter monsoon and Arctic Oscillation. *Geophys. Res. Lett.,* **28,** 2073–2076.

Graham, N., 1994: Decadal-scale climate variability in the tropical and North Pacific during the 1970s and 1980s: Observations and model results. *Climate Dyn.,* **10,** 135–162.

Guo, Q. Y., 1994: Relationship between the variations of East Asian winter monsoon and temperature anomalies in China (in Chinese). *Quart. J. Appl. Meteor.,* **5,** 218–225.

He, S., 2013: Reduction of the East Asian winter monsoon interannual variability after the mid-1980s and possible cause. *Chin. Sci. Bull.,* **58,** 1131–1138.

——, and H. Wang, 2012: An integrated East Asian winter monsoon index and its interannual variability (in Chinese). *Chin. J. Atmos. Sci.,* **36,** 523–538.

——, ——, and J. Liu, 2013: Changes in the relationship between ENSO and Asia–Pacific midlatitude winter atmospheric circulation. *J. Climate,* **26,** 3377–3393.

Holton, J. R., 1992: *An Introduction to Dynamic Meteorology.* 3rd ed. Academic Press, 511 pp.

Jeong, J. H., T. Ou, H. W. Linderholm, B. M. Kim, S. J. Kim, J. S. Kug, and D. Chen, 2011: Recent recovery of the Siberian high intensity. *J. Geophys. Res.,* **116,** D23102, doi:10.1029/2011JD015904.

Jhun, J. G., and E. J. Lee, 2004: A new East Asian winter monsoon index and associated characteristics of the winter monsoon. *J. Climate,* **17,** 711–726.

Kanamitsu, M., W. Ebisuzaki, J. Woollen, S.-K. Yang, J. J. Hnilo, M. Fiorino, and G. L. Potter, 2002: NCEP–DOE AMIP-II Reanalysis (R-2). *Bull. Amer. Meteor. Soc.,* **83,** 1631–1644.

Kerr, R. A., 2000: A North Atlantic climate pacemaker for the centuries. *Science,* **288,** 1984–1985.

Kirtman, B. P., and P. S. Schopf, 1998: Decadal variability in ENSO predictability and prediction. *J. Climate,* **11,** 2804–2822.

Kumar, K. K., B. Rajagopalan, and M. A. Cane, 1999: On the weakening relationship between the Indian monsoon and ENSO. *Science,* **284,** 2156–2159.

Lau, K. M., and M. T. Li, 1984: The monsoon of East Asia and its global associations—A survey. *Bull. Amer. Meteor. Soc.,* **65,** 114–125.

Lau, N.-C., 1997: Interactions between global SST anomalies and the midlatitude atmospheric circulation. *Bull. Amer. Meteor. Soc.,* **78,** 21–33.

——, and M. J. Nath, 1996: The role of the ''atmospheric bridge'' in linking tropical Pacific ENSO events to extratropical SST anomalies. *J. Climate,* **9,** 2036–2057.

Lee, T., and M. J. McPhaden, 2008: Decadal phase change in large-scale sea level and winds in the Indo-Pacific region at the end of the 20th century. *Geophys. Res. Lett.,* **35,** L01605, doi:10.1029/2007GL032419.

Li, C. Y., 1990: Interaction between anomalous winter monsoon in East Asia and El Niño events. *Adv. Atmos. Sci.,* **7,** 36–46.

Li, F., and H. Wang, 2012a: Predictability of the East Asian winter monsoon interannual variability as indicated by the DEMETER CGCMS. *Adv. Atmos. Sci.,* **29,** 441–454.

——, and ——, 2012b: Relationship between Bering Sea ice cover and East Asian winter monsoon year-to-year variations. *Adv. Atmos. Sci.,* **30,** 48–56.

——, and ——, 2013: Autumn sea ice cover, winter Northern Hemisphere annular mode, and winter precipitation in Eurasia. *J. Climate,* **26,** 3968–3981.

Li, S., and G. T. Bates, 2007: Influence of the Atlantic multidecadal oscillation on the winter climate of east China. *Adv. Atmos. Sci.,* **24,** 126–135.

Li, Y. Q., and S. Yang, 2010: A dynamical index for the East Asian winter monsoon. *J. Climate,* **23,** 4255–4262.

Linkin, M. E., and S. Nigam, 2008: The North Pacific Oscillation–west Pacific teleconnection pattern: Mature-phase structure and winter impacts. *J. Climate,* **21,** 1979–1997.

Mantua, N. J., S. R. Hare, Y. Zhang, J. M. Wallace, and R. C. Francis, 1997: A Pacific interdecadal climate oscillation with impacts on salmon production. *Bull. Amer. Meteor. Soc.,* **78,** 1069–1079.

Mitchell, T. D., and P. D. Jones, 2005: An improved method of constructing a database of monthly climate observations and associated high-resolution grids. *Int. J. Climatol.,* **25,** 693–712.

Namias, J., X. Yuan, and D. Cayan, 1988: Persistence of North Pacific sea surface temperature and atmospheric flow patterns. *J. Climate,* **1,** 682–703.

Nitta, T., and S. Yamada, 1989: Recent warming of tropical sea surface temperature and its relationship to the Northern Hemisphere circulation. *J. Meteor. Soc. Japan,* **67,** 375–383.

Overland, J. E., J. M. Adams, and N. A. Bond, 1999: Decadal variability of the Aleutian low and its relation to high-latitude circulation. *J. Climate,* **12,** 1542–1548.

Smith, T. M., R. W. Reynolds, T. C. Peterson, and J. Lawrimore, 2008: Improvements to NOAA's historical merged land–ocean surface temperature analysis (1880–2006). *J. Climate,* **21,** 2283–2296.

Sun, B. M., and C. Y. Li, 1997: Relationship between the disturbances of East Asian trough and tropical convective activities in boreal winter. *Chin. Sci. Bull.,* **42,** 500–504.

——, and H. Wang, 2012: Larger variability, better predictability? *Int. J. Climatol.,* **33,** 2341–2351, doi:10.1002/joc.3582.

Sun, J., and H. Wang, 2006: Relationship between Arctic Oscillation and Pacific decadal oscillation on decadal timescale. *Chin. Sci. Bull.,* **51,** 75–79.

Tanaka, H., N. Ishizaki, and A. Kitoh, 2004: Trend and interannual variability of Walker, monsoon and Hadley circulations defined by velocity potential in the upper troposphere. *Tellus,* **56A,** 250–269.

Thompson, D. W. J., and J. M. Wallace, 1998: The Arctic Oscillation signature in the wintertime geopotential height and temperature fields. *Geophys. Res. Lett.,* **25,** 1297–1300.

——, and ——, 2000: Annular modes in the extratropical circulation. Part I: Month-to-month variability. *J. Climate,* **13,** 1000–1016.

Trenberth, K. E., 1990: Recent observed interdecadal climate changes in the Northern Hemisphere. *Bull. Amer. Meteor. Soc.,* **71,** 988–993.

——, and J. W. Hurrell, 1994: Decadal atmosphere-ocean variations in the Pacific. *Climate Dyn.,* **9,** 303–319.

Wallace, J. M., and D. S. Gutzler, 1981: Teleconnections in the geopotential height field during the Northern Hemisphere winter. *Mon. Wea. Rev.,* **109,** 784–812.

Wang, B., Ed., 2006: *The Asian Monsoon*. Springer Praxis, 799 pp.

——, R. Wu, and X. Fu, 2000: Pacific–East Asian teleconnection: How does ENSO affect East Asian climate? *J. Climate,* **13,** 1517–1536.

Wang, H., 2001: The weakening of the Asian monsoon circulation after the end of 1970's. *Adv. Atmos. Sci.,* **18,** 376–386.

——, 2002: The instability of the East Asian summer monsoon–ENSO relations. *Adv. Atmos. Sci.,* **19,** 1–11.

——, and S. He, 2012: Weakening relationship between East Asian winter monsoon and ENSO after mid-1970s. *Chin. Sci. Bull.,* **57,** 3535–3540.

——, E. Yu, and S. Yang, 2011: An exceptionally heavy snowfall in northeast China: Large-scale circulation anomalies and hindcast of the NCAR WRF model. *Meteor. Atmos. Phys.,* **113,** 11–25.

Wang, L., and W. Chen, 2010: How well do existing indices measure the strength of the East Asian winter monsoon? *Adv. Atmos. Sci.,* **27,** 855–870.

——, ——, and R. H. Huang, 2008: Interdecadal modulation of PDO on the impact of ENSO on the East Asian winter monsoon. *Geophys. Res. Lett.,* **35,** L20702, doi:10.1029/2008GL035287.

——, ——, W. Zhou, and R. Huang, 2009: Interannual variations of East Asian trough axis at 500 hPa and its association with the East Asian winter monsoon pathway. *J. Climate,* **22,** 600–614.

——, ——, ——, J. C. L. Chan, D. Barriopedro, and R. Huang, 2010: Effect of the climate shift around mid 1970s on the relationship between wintertime Ural blocking circulation and East Asian climate. *Int. J. Climatol.,* **30,** 153–158.

Watanabe, M., and T. Nitta, 1999: Decadal changes in the atmospheric circulation and associated surface climate variations in the Northern Hemisphere winter. *J. Climate,* **12,** 494–510.

Wei, K., W. Chen, and W. Zhou, 2011: Changes in the East Asian cold season since 2000. *Adv. Atmos. Sci.,* **28,** 69–79.

Wu, B., and R. H. Huang, 1999: Effects of the extremes in the North Atlantic Oscillation on East Asia winter monsoon (in Chinese). *Chin. J. Atmos. Sci.,* **26,** 641–651.

——, and J. Wang, 2002: Winter Arctic Oscillation, Siberian high and East Asian winter monsoon. *Geophys. Res. Lett.,* **29,** 1897, doi:10.1029/2002GL015373.

Wu, R., and B. Wang, 2002: A contrast of the East Asian summer monsoon–ENSO relationship between 1962–77 and 1978–93. *J. Climate,* **15,** 3266–3279.

Zhang, R., A. Sumi, and M. Kimoto, 1996: Impact of El Niño on the East Asian monsoon: A diagnostic study of the '86/87 and '91/92 events. *J. Meteor. Soc. Japan,* **74,** 49–62.

Zhang, Y., K. R. Sperber, and J. S. Boyle, 1997: Climatology and interannual variation of the East Asian winter monsoon: Results from the 1979–95 NCEP/NCAR reanalysis. *Mon. Wea. Rev.,* **125,** 2605–2619.

Zhou, W., C. Li, and X. Wang, 2007a: Possible connection between Pacific oceanic interdecadal pathway and East Asian winter monsoon. *Geophys. Res. Lett.,* **34,** L01701, doi:10.1029/2006GL027809.

——, X. Wang, T. J. Zhou, C. Li, and J. C. L. Chan, 2007b: Interdecadal variability of the relationship between the East Asian winter monsoon and ENSO. *Meteor. Atmos. Phys.,* **98,** 283–293.

——, J. C. L. Chan, W. Chen, J. Ling, J. G. Pinto, and Y. Shao, 2009: Synoptic-scale controls of persistent low temperature and icy weather over southern China in January 2008. *Mon. Wea. Rev.,* **137,** 283–293.